Self-Initiating MUSIC-Based Direction Finding in Underwater Acoustic Particle Velocity-Field Beamspace

Kainam T. Wong, *Member, IEEE,* and Michael D. Zoltowski, *Fellow, IEEE*

***Abstract*—This paper introduces a novel blind MUSIC-based (MUltiple SIgnal Classification) source localization algorithm applicable to an arbitrarily spaced three-dimensional array of vector hydrophones, each of which comprises two or more co-located and orthogonally oriented velocity hydrophones plus an optional pressure hydrophone. This proposed algorithm: 1) exploits the incident sources' angular diversity in the underwater acoustic particle velocity field; 2) adaptively forms velocity-field beams at each vector-hydrophone; 3) uses ESPRIT to self-generate coarse estimates of the sources' arrival angles to start off its MUSIC-based iterative search with no *a priori* source information; and 4) automatically pairs the x-axis direction-cosine estimates with the y-axis direction-cosine estimates. Simulation results verify the efficacy of this proposed scheme.**

***Index Terms*—Acoustic interferometry, acoustic signal processing, acoustic velocity measurement, array signal processing, blind estimation, direction of arrival estimation, sonar arrays, underwater acoustic arrays.**

I. Basic Ideas Underlying the New Algorithm

A. MUSIC-Based Parameter Estimation

MUSIC (MUltiple SIgnal Classification) [5] represents a highly popular eigenstructure (subspace) direction-finding (DF) method applicable to arrays of irregularly spaced sensors. MUSIC forms a spectrum using the noise-subspace eigenvectors of the data correlation matrix and then searches iteratively for nulls in this spectrum. MUSIC, thus, performs an M-dimensional iterative search for K extrema of a scalar function to estimate the M parameters of all K incident sources. Relative to the optimum maximum-likelihood (ML) parameter estimation method, eigenstructure methods: 1) demand less computation; 2) do not require *a priori* information of the joint probability density relating all sources and noises but only the noise's second-order statistics; 3) yield asymptotically unbiased and efficient estimates of the directions-of-arrival (DOA); and 4) produce at moderate signal-to-noise ratio (SNR) estimation performance comparable to the optimal methods. Irregular inter-hydrophone spacing frequently arises, for example, when multiple identical sonobuoy subarrays are scattered over a wide area, in sparse arrays for aperture extension, in log-periodic arrays for frequency-invariant beamforming, and in conformal arrays. For such irregularly spaced arrays of pressure hydrophones, ESPRIT [7]—the other popular eigenstructure method—cannot effectively process the collected data from *all* pressure hydrophones. This is because ESPRIT requires the overall array to be decomposable into two identical but translated subarrays, a condition violated by the geometric irregularity of the arbitrarily spaced array. However, ESPRIT will be used in this algorithm to process the data from pairs of vector hydrophones to generate coarse arrival angle estimates to initiate MUSIC. ESPRIT can be so used despite the array's geometric irregularity because of the vector nature of the vector hydrophones.

This work represents the first paper relating the MUSIC algorithm to an irregular array of vector hydrophones. This present algorithm further distinguishes itself from other beamspace MUSIC algorithms [8]–[10] in several regards: 1) beams are formed in the velocity-field domain; 2) these velocity-field beams are formed *blindly* using no *a priori* source information; and 3) coarse estimates of the direction cosine are derived to start off MUSIC's iterative search. This present algorithm does not require any *a priori* source information; however, if any such information becomes available, it would be possible to incorporate techniques presented in [8]–[10] to form beams in the spatial domain as well.

B. Vector Hydrophones

This proposed method is applicable to any irregularly spaced array of vector hydrophones, each of which comprises two or three[1] identical co-located but orthogonally oriented velocity hydrophones plus an optional co-located pressure hydrophone. Each velocity hydrophone has an intrinsically directional response to the incident underwater acoustic wavefield, measuring only one Cartesian component of the incident three-dimensional (3-D) underwater acoustic particle velocity field. Each vector hydrophone (constructed with three orthogonal velocity hydrophones) thus measures all three Cartesian components of the incident acoustic particle velocity-field. The kth incident signal would effect a steering vector whose components are the signal's three Cartesian direction-cosines $\{u(\theta_k, \phi_k) = \sin\theta_k \cos\phi_k, v(\theta_k, \phi_k) =$

Manuscript received October 14, 1997; revised June 22, 1999. This work was supported by the National Science Foundation under Grant MIPS-9320890, the Air Force Office of Scientific Research under Contract F49620-95-1-0367, and the Army Research Office Focused Research Initiative under Grant DAAH04-95-1-0246. A portion of this paper was presented at the 1997 IEEE International Symposium on Circuits & Systems.

K. T. Wong is with the Department of Electronic Engineering, Chinese University of Hong Kong, Shatin, NT, Hong Kong.

M. D. Zoltowski is with the School of Electrical and Computer Engineering, Purdue University, West Lafayette, IN 47907-1285 USA.

Publisher Item Identifier S 0364-9059(00)03368-9.

[1]To avoid directly dealing with the vertical component of the underwater acoustical particle motion, the vector hydrophone may comprise only two horizontally oriented velocity hydrophones plus a pressure hydrophone. This allows the measured ocean acoustics to be modeled as rectilinear.

$\sin\theta_k \sin\phi_k, w(\theta_k) = \cos\theta_k, k = 1, \cdots, K\}$ where ϕ_k symbolizes the kth source's azimuth angle and θ_k represents the elevation angle. The vector hydrophone's unique array manifold is pivotal to the efficacy of this proposed approach. The Swallow floats [11], one example of a freely drifting array of vector hydrophones, are neutrally buoyant and may be ballasted to any desired depth in the ocean. The DIFAR array [12], [13], a uniform vertical array with flux-gate compasses to measure the orientation of the horizontal velocity hydrophones, exemplifies another possible construction of vector hydrophones. Velocity-hydrophone technology has been available for some time [1] and continues to attract attention in the field of underwater acoustics [29]. Many different types of velocity hydrophones are available [3] and have been constructed using a variety of technologies, with designs ranging from mechanically-based [4] to optically-based [6] to derivative-based [16]. This recognition of the vector-field nature (i.e., the acoustic particle velocity field) of the underwater acoustic wavefield distinguishes this algorithm from more customary source localization methods deploying pressure hydrophones and treating the underwater acoustic wavefield as merely a scalar wavefield (i.e., a pressure field).

Velocity hydrophones have been used in several earlier signal processing papers. D'Spain *et al.* [13] and Hawkes and Nehorai [28] investigated Capon spectrum estimation along predetermined spatial direction for an array of vector hydrophones. The vector-hydrophone beam pattern is analyzed by Wong and Chi [31]. Shchurov *et al.* [14] used vector hydrophones to measure ambient noise but not for source direction finding. Nehorai and Paldi [16] developed a measurement model of the vector hydrophone and stated that the normalized vector-hydrophone array manifold contains the direction-cosines as its components. Nehorai and Paldi [16] also proposed a scalar performance measure [the mean square angular error (MSAE)], derived a compact expression and a bound for the asymptotic MSAE for the vector hydrophone, and proposed a fast wide-band estimator of the arrival angles in a single-source scenario using one vector hydrophone. Hochwald and Nehorai [21] determined the maximum number of sources uniquely identifiable with a single vector hydrophone. Hawkes and Nehorai also derived theoretical performance bounds for direction finding and beamforming using an array of vector hydrophones [28], [18] and analyzed underwater acoustic boundary conditions for hull-mounted [19] and surface-mounted [20] vector hydrophones. Wong and Zoltowski used the ESPRIT-based normalization DOA-estimator on a single vector hydrophone [23], [30] and to extend array aperture beyond half-wavelength spacing for a sparse but regularly spaced multi-element planar array of vector hydrophones [24]. Wong and Zoltowski also devised a Root-MUSIC direction-finding algorithm applicable to *uniformly* spaced velocity hydrophones [29]. In contrast, this proposed method performs direction finding in the acoustic particle velocity-field beamspace for arbitrarily spaced vector hydrophones using a self-initiating MUSIC-based iterative method.

C. Acoustic Particle Velocity-Field Beamspace

Considering each vector hydrophone as a subarray unit, identical velocity-field beams in two- (angular-)dimensional space may be formed at each individual vector hydrophone. These vector-hydrophone-based beams, to be formed by linearly constrained minimum variance (LCMV) beamforming, may be directed to any azimuth-elevation direction to pass only one signal-of-interest while nulling out all interference. This would eliminate many local optima in MUSIC's iterative search and thus facilitate more speedy and more robust convergence to the global optimum.

In order to specify the linear constraints used to construct this LCMV beamformer, it would be necessary to estimate each source's respective vector hydrophone steering vector. This may be accomplished by applying TLS-ESPRIT—a total least squares refinement of ESPRIT [7]—to a pair of vector hydrophones, which effectively embody two identical but spatially translated three-element subarrays, the data collected from which form an ESPRIT matrix-pencil pair. The lower-dimensional eigenvectors (*not* the signal-subspace nor the null-space eigenvectors of the data correlation matrix) generated in the final stage of TLS-ESPRIT are used to decouple the element-space signal-subspace eigenvectors to yield an estimate of each source's vector-hydrophone steering vector, which may in turn be used as linear constraints for LCMV beamforming over the two-dimensional (2-D) parameter-space of the azimuth and the elevation.

D. Blind Estimation via Self-Initiating MUSIC

MUSIC, however, performs a computationally expensive iterative optimization search over a multidimensional parameter-space. Whether this optimization converges to the global optimum and how fast this iterative search converges depend very much on the proximity of the initial parameter values to the true global optimum. Without *a priori* information on the incident sources, initial estimates are generally unobtainable. One advantage provided by this proposed method is the capability to self-generate such initial estimates *blindly* without any *a priori* information. Coarse DOA estimates are herein derived based on the vector hydrophone's unique array manifold, which contains an incident source's all three Cartesian velocity components. Such estimates of the kth source's steering vector, already available from TLS-ESPRIT as explained earlier, when normalized produce estimates of the source's Cartesian coordinate direction-cosines, $\{\hat{u}_k^{\rm coar}, \hat{v}_k^{\rm coar}, \hat{w}_k^{\rm coar}\}$, which can serve as "coarse" estimates to start off MUSIC's iterative search. In essence, the deployment of multiple spatially displaced vector hydrophones allows two separate independent approaches to estimate the DOA's—via the normalization DOA estimator [16] at each vector hydrophone and via an iterative search over the multivector-hydrophone array manifold parameterized by the inter-vector-hydrophone phase delays. The high variances of these normalization DOA estimates (relative to the direction-cosine estimates to be derived through acoustic particle velocity-field beamspace MUSIC's iterative search) are intuitively explainable as due to its derivation based on information from a single vector hydrophone, which has no effective geometric aperture because of its point-like geometry. In contrast, MUSIC's estimates benefit from the nonzero spatial extent of the full array aperture.

E. Automatic Pairing of Direction-Cosine Estimates

A nontrivial pairing problem with the direction-cosine estimates would ordinarily arise with geometrically separable array configurations using pressure hydrophones, but not in the present case with vector hydrophones. This present algorithm automatically pairs estimates of the x-axis direction-cosines with those along the y axis. This pairing problem is nontrivial because there does not exist any fundamental algebraic theorem nor any general algorithm for such a 2-D problem. What do exist are numerous algorithms that apply only to arrays that separately estimate the two sets of direction-cosines and then pair them. For example, in cross-shaped, L-shaped, or planar arrays, hydrophones displaced along the x axis leads to estimates of the direction-cosines along the x axis; hydrophones displaced along the y axis leads to estimates of direction-cosines along the y axis. However, even with such separable array configurations, there remains the aforementioned nontrivial problem to pair the x-axis direction-cosine estimates with the y-axis direction-cosine estimates. In contrast, this proposed algorithm has already automatically resolved this pairing problem because the direction-cosine estimates are already correctly paired in the normalization estimates.

F. Organization of this Paper

The remainder of this paper will first develop the proposed self-initiating MUSIC-based azimuth/elevation source localization algorithm for an array of arbitrarily spaced vector hydrophones, each of which is made of three identical and co-located but orthogonally oriented velocity hydrophones; this version of the proposed algorithm can handle up to two incident sources. Section III-E1 then extends the algorithm for vector hydrophones made of the aforementioned velocity-hydrophone triad plus an additional co-located pressure hydrophone (to distinguish between acoustic compressions and dilations); this version of the proposed algorithm can handle up to three incident sources. Section III-E2 modifies the algorithm for vector hydrophones made of only two horizontally and orthogonally oriented velocity hydrophones plus an additional co-located pressure hydrophone; this version of the proposed algorithm can handle up to two incident sources. The elimination of the vertically oriented velocity hydrophone will allow actual ocean acoustics to be better modeled as rectilinear. Section III-F presents a variation of the schemes in Section III-E to handle more than three sources.

II. Data Model for Irregularly Spaced Vector Hydrophones

Uncorrelated narrow-band[2] underwater acoustic plane-waves impinge from one side[3] of an array of vector hydrophones located irregularly in a 3-D region. Each vector hydrophone consists of three spatially co-located but orthogonally oriented velocity hydrophones. The kth impinging source has the following 3×1 vector-hydrophone array manifold [16]:

$$\boldsymbol{a}_k \stackrel{\text{def}}{=} \boldsymbol{a}(\theta_k,\, \phi_k) \stackrel{\text{def}}{=} \begin{bmatrix} u(\theta_k,\, \phi_k) \\ v(\theta_k,\, \phi_k) \\ w(\theta_k) \end{bmatrix} \stackrel{\text{def}}{=} \begin{bmatrix} u_k \\ v_k \\ w_k \end{bmatrix} \stackrel{\text{def}}{=} \begin{bmatrix} \sin\theta_k \cos\phi_k \\ \sin\theta_k \sin\phi_k \\ \cos\theta_k \end{bmatrix} \tag{1}$$

where $0 \leq \theta_k < \pi/2$ symbolizes the kth source's elevation angle measured from the vertical z axis, $0 \leq \phi_k < 2\pi$ denotes the kth source's azimuth angle, $u_k \stackrel{\text{def}}{=} \sin\,\theta_k\, \cos\,\phi_k$ represents the direction-cosine along the x axis, $v_k \stackrel{\text{def}}{=} \sin\,\theta_k\, \sin\,\phi_k$ symbolizes the direction-cosine along the y axis, and $w_k \stackrel{\text{def}}{=} \cos\,\theta_k$ denotes the direction-cosine along the z axis.

There are two essential observations about this array manifold. First, each vector hydrophone yields a 3×1 steering vector—each vector hydrophone effectively embodies a three-element subarray in and of itself. Second, the normalized steering vector $\boldsymbol{a}_k$ uniquely determines a broad-band or narrow-band source's DOA. Thus, if the steering vectors of all impinging sources can be estimated from the received data, then the signal-of-interests' DOA's can be estimated by simply normalizing their respective steering vector estimates.

The spatial phase factor for the kth incident source at the lth vector hydrophone located at $(x_l,\, y_l,\, z_l)$ is

$$\begin{aligned} q_l(\theta_k,\, \phi_k) &\stackrel{\text{def}}{=} e^{j2\pi((x_l u_k + y_l v_k + z_l w_k)/\lambda)} \\ &= \underbrace{e^{j2\pi(x_l u_k/\lambda)}}_{\stackrel{\text{def}}{=} q_l^x(u_k)} \underbrace{e^{j2\pi(y_l v_k/\lambda)}}_{\stackrel{\text{def}}{=} q_l^y(v_k)} \underbrace{e^{j2\pi(z_l w_k/\lambda)}}_{\stackrel{\text{def}}{=} q_l^z(w_k)}. \end{aligned} \tag{2}$$

The kth signal impinging upon the lth vector hydrophone at time t thus registers the three-component vector measurement

$$\begin{aligned} &\boldsymbol{a}(\theta_k,\, \phi_k) s_k(t) q_l(\theta_k,\, \phi_k), \\ &\quad \text{where} \quad s_k(t) \stackrel{\text{def}}{=} \sqrt{\mathcal{P}_k}\, \sigma_k(t) e^{j(2\pi(c/\lambda)t + \varphi_k)} \end{aligned} \tag{3}$$

where $\mathcal{P}_k$ denotes the kth signal's power, $\sigma_k(t)$ is a zero-mean unit-variance complex random process, λ is the signals' wavelength, c is the propagation speed, and φ_k is the kth signal's uniformly-distributed random carrier phase.

With a total of $K \leq 2$ co-channel signals, the lth vector hydrophone has the 3×1 vector measurement

$$\begin{aligned} \boldsymbol{z}_l(t) &= \sum_{k=1}^{K} \underbrace{\boldsymbol{a}(\theta_k,\, \phi_k) q_l(\theta_k,\, \phi_k)}_{\stackrel{\text{def}}{=} \boldsymbol{a}_l(\theta_k,\, \phi_k)} s_k(t) + \boldsymbol{n}_l(t), \\ l &= 1,\, \cdots,\, L. \end{aligned} \tag{4}$$

(The above $K \leq 2$ source maximum limit may readily be raised to $3\tilde{L} - 1$ by replacing each vector hydrophone with a subarray of $\tilde{L}$ vector hydrophones. Such subarrays may be arbitrarily configured so long as the same subarray configuration is used at all locations. This extension will be discussed in detail in the next section.)

[2]These incident signals are narrow-band in that their bandwidths are very small compared to the inverse of the wavefronts' transit times across the array. The case involving broad-band signals may be reduced to a set of narrow-band problems using a comb of narrow-band filters.

[3]The sources may impinge from both sides of the array if the vector hydrophone is constructed using the three velocity hydrophones plus a pressure hydrophone.

For the entire arbitrarily spaced vector-hydrophone array,[4] there exists a $3L \times 1$ vector measurement at each t

$$\boldsymbol{z}(t) \stackrel{\text{def}}{=} \begin{bmatrix} \boldsymbol{z}_1(t) \\ \vdots \\ \boldsymbol{z}_L(t) \end{bmatrix} = \sum_{k=1}^{K} s_k(t)\boldsymbol{q}(u_k, v_k) \otimes \boldsymbol{a}(\theta_k, \phi_k) + \boldsymbol{n}(t) = \boldsymbol{A}\boldsymbol{s}(t) + \boldsymbol{n}(t) \tag{5}$$

where $\boldsymbol{A}$ is the $3L \times K$ matrix

$$\boldsymbol{A} \stackrel{\text{def}}{=} [\boldsymbol{q}(u_1, v_1) \otimes \boldsymbol{a}(\theta_1, \phi_1), \cdots, \boldsymbol{q}(u_K, v_K) \otimes \boldsymbol{a}(\theta_K, \phi_K)] \tag{6}$$

and

$$\boldsymbol{s}(t) \stackrel{\text{def}}{=} \begin{bmatrix} s_1(t) \\ \vdots \\ s_K(t) \end{bmatrix} \quad \boldsymbol{n}(t) \stackrel{\text{def}}{=} \begin{bmatrix} \boldsymbol{n}_1(t) \\ \vdots \\ \boldsymbol{n}_L(t) \end{bmatrix} \quad \boldsymbol{q}(u_k, v_k) \stackrel{\text{def}}{=} \begin{bmatrix} e^{j2\pi((x_1 u_k + y_1 v_1 + z_1 w_k)/\lambda)} \\ \vdots \\ e^{j2\pi((x_L u_k + y_L v_k + z_L w_k)/\lambda)} \end{bmatrix} \tag{7}$$

where $\otimes$ denotes the Kronecker product, $\boldsymbol{n}_l(t)$ symbolizes the 3×1 complex-valued zero-mean additive white noise vector at the lth vector hydrophone, and $w_k = \sqrt{1 - u_k^2 - v_k^2}$ for $k = 1, \cdots, K$. With a total of $N > K \leq 2$ snapshots taken at the distinct times $\{t_n, n = 1, \cdots, N\}$, the vector-hydrophone direction-finding problem.[5] is to determine all $\{\theta_k, \phi_k, k = 1, \cdots, K\}$ from the $3L \times N$ data set

$$\boldsymbol{Z} \stackrel{\text{def}}{=} \begin{bmatrix} \boldsymbol{Z}_1 \\ \vdots \\ \boldsymbol{Z}_L \end{bmatrix} = \begin{bmatrix} \boldsymbol{z}_1(t_1) & \dots & \boldsymbol{z}_1(t_N) \\ \vdots & & \vdots \\ \boldsymbol{z}_L(t_1) & \dots & \boldsymbol{z}_L(t_N) \end{bmatrix} \tag{8}$$

where the $3 \times N$ submatrices $\{\boldsymbol{Z}_l, l = 1, \cdots, L\}$ correspond to measurements at the lth vector hydrophone.

III. Self-Initiating MUSIC-Based DF in Acoustic Particle Velocity-Field Beamspace

A. Eigen-Decomposition of Sampled Data

In eigenstructure (subspace) DF methods (such as MUSIC), the overall sample correlation matrix $\boldsymbol{Z}\boldsymbol{Z}^H$ (which embodies a maximum likelihood (ML) estimate of the true sample correlation matrix if the additive noise is Gaussian) is decomposed into a K-dimensional signal subspace and a $(L - K)$-dimensional noise subspace. MUSIC derives a null spectrum (or source spectrum) parameterized by the direction-cosines and then identifies the deepest nulls in this null spectrum (or peaks for the source spectrum) to estimate the arrival angles. Hence, MUSIC performs a 2-D search for K extrema of a scalar function to estimate the azimuth and elevation angles of all K incident sources. Let $\boldsymbol{E}_s$ symbolize the $3L \times K$ matrix composed of the K eigenvectors corresponding to the K largest eigenvalues of the $3L \times 3L$ sample data correlation matrix, and let $\boldsymbol{E}_n$ denote the $3L \times (3L - K)$, matrix composed of the remaining $3L - K$ eigenvectors of $\boldsymbol{Z}\boldsymbol{Z}^H$:

$$\boldsymbol{R}_{zz} = \boldsymbol{Z}\boldsymbol{Z}^H = \frac{1}{N}\sum_{i=1}^{N} \boldsymbol{z}(t_i)\boldsymbol{z}^H(t_i) = \boldsymbol{E}_s\boldsymbol{D}_s\boldsymbol{E}_s^H + \boldsymbol{E}_n\boldsymbol{D}_n\boldsymbol{E}_n^H \tag{9}$$

where

$$\boldsymbol{E}_s \approx \boldsymbol{A}\boldsymbol{T} = [\boldsymbol{q}(u_1, v_1) \otimes \boldsymbol{a}(\theta_1, \phi_1), \cdots, \boldsymbol{q}(u_K, v_K) \otimes \boldsymbol{a}(\theta_K, \phi_K)]\boldsymbol{T}. \tag{10}$$

$\boldsymbol{D}_s$ symbolizes a $K \times K$ diagonal matrix whose diagonal entries embody the K largest eigenvalues, and $\boldsymbol{D}_n$ represents a $(3L - K) \times (3L - K)$ diagonal matrix whose diagonal entries contain the $3L - K$ smallest eigenvalues, and $\boldsymbol{T}$ denotes an unknown but nonsingular $K \times K$ coupling matrix. $\boldsymbol{T}$ is nonsingular because both $\boldsymbol{E}_s$ and $\boldsymbol{A}$ are full rank. If there existed no noise, or an infinite number of snapshots were available, the above approximation would become an exact identity.

B. Blind Beamforming in the Acoustic Particle Velocity Field

Velocity-field beamforming removes those spectral optima corresponding to interfering sources by nulling out all but one signal-of-interest at a time, thereby facilitating MUSIC's iterative search for a speedy convergence to the global optimum. Prior to this acoustic particle velocity-field beamforming step, data dimensions have already been reduced by the eigen-decomposition step in (9) to (10) from $3L \times N$ to $3L \times K$. By constructing an identical beam out of each vector hydrophone of the irregularly spaced 3-D array, velocity-field beamforming further reduces these data dimensions to $L \times K$. Moreover, because the vector hydrophone's array manifold depends on both azimuth and elevation, spatial beams with two angular dimensions may be formed out of a solitary vector hydrophone. This implies, among other advantages, that two-spatial-dimensional beamforming and DF may be performed with only a one-dimensional array of vector hydrophones.

LCMV [2] is a statistically optimal beamforming technique that allows extensive control of beamformer response by a set of linear constraints, which may be set to pass (with specified gain and phase) signals from favored directions or to block interferences from other directions and to minimize output variance. LCMV has effects similar to constraining the coefficients of a finite impulse response (FIR) filter to produce a specified set of spectral peaks and nulls.

[4]The following algorithmic development assumes that all L vector hydrophones are identically oriented. A simple correctional procedure is presented in [25] to accommodate any nonidentical orientation among the L vector hydrophones

[5]Although the proposed algorithm will be presented in the batch processing mode, real-time adaptive implementations of this present algorithm may readily be realized for nonstationary environments using the fast recursive eigen-decomposition updating methods such as those in [15] and [17].

The LCMV beamformer weights passing the kth source but nulling all other $K-1$ sources may be derived as

$$\boldsymbol{w}_k = \boldsymbol{R}_{vh}^{-1}\boldsymbol{C}\left(\boldsymbol{C}^H\boldsymbol{R}_{vh}^{-1}\boldsymbol{C}\right)^{-1}\boldsymbol{e}_k \tag{11}$$

where

$$\boldsymbol{R}_{vh} \stackrel{\text{def}}{=} \sum_{k=1}^{K} \hat{\boldsymbol{a}}_k \hat{\boldsymbol{a}}_k^H \tag{12}$$

$$\boldsymbol{C} \stackrel{\text{def}}{=} [\hat{\boldsymbol{a}}_1 \ \vdots \ \cdots \ \vdots \ \hat{\boldsymbol{a}}_K] \tag{13}$$

and $\{\hat{\boldsymbol{a}}_k, k=1,\cdots,K\}$ embody entities to be estimated. Note that the K columns of the constraint matrix $\boldsymbol{C}$ simply correspond to the K sources' estimated array manifolds, and $\boldsymbol{e}_k$ is a $K\times 1$ vector with all zeros except a 1 at the kth position to indicate that only the kth source is to be passed. This $\boldsymbol{w}_k$ minimizes $\boldsymbol{w}_k^H\boldsymbol{R}_{vh}\boldsymbol{w}_k$ (i.e., the output variance or power) while satisfying the constraints $\boldsymbol{C}^H\boldsymbol{w}_k = \boldsymbol{e}_k$. Note that these acoustic particle velocity-field beams have been formed without explicit estimation of the arrival angles.

This 3×1 LCMV acoustic particle velocity-field beamforming weight vector $\boldsymbol{w}_k$ is to be applied identically to each $3\times K$ sector of the $3L\times K$ signal-subspace eigenvector matrix of (10) as follows:

$$\boldsymbol{E}_{b_k} \stackrel{\text{def}}{=} (\boldsymbol{I}_L \otimes \boldsymbol{w}_k^H)\boldsymbol{E}_s \tag{14}$$

where $\boldsymbol{E}_{b_k}$ denotes the kth source's $L\times K$ velocity-field beamformer output, passing only the kth source but nulling all other $K-1$ sources. This $L\times K$ velocity-field beamformer output will then be used in a 2-D DOA search to be discussed in Section III-C. Note that each signal-of-interest would have its own $\boldsymbol{w}_k$, $\boldsymbol{E}_{b_k}$, and 2-D iterative search.

The impinging sources' spatial diversity is exploited by this univector-hydrophone-based beamformer in a way fundamentally different with a conventional phased array of displaced pressure hydrophones. In the latter case, the spatial diversity among incident sources is encapsulated in the spatial phase factors between the phased array's spatially displaced pressure hydrophones. In contrast, no such spatial phase factors exist among each vector hydrophone's component hydrophones because all three velocity hydrophones are spatially co-located. The Vandermonde structure in the array manifold of a uniformly spaced array of identical pressure hydrophones no longer exists *within* a vector hydrophone. Instead, the sources' spatial diversity is directly encapsulated by the vector hydrophone in the scalar response of each component hydrophone comprising the vector hydrophone. Univector-hydrophone beamforming, thus, embodies a kind of acoustic particle velocity-field weighting, fundamentally distinct from the phased array's spatial filtering. Note also that *spatial* beamforming techniques [8]–[10] mentioned earlier could be applied to further reduce the dimension of this $L\times K$ velocity-field beamspace data set when *a priori* DOA information on the incident sources are available.

C. Estimation of Vector-Hydrophone Steering Vectors

The blind beamforming procedure suggested in the preceding subsection needs $\{\hat{\boldsymbol{a}}_k, k=1,\cdots,K\}$, which may be derived using TLS-ESPRIT [7]. ESPRIT exploits the translational invariance between two identical subarrays translated by a known separation Δ. Because each vector hydrophone embodies a three-component subarray, any two vector hydrophones may be considered as an ESPRIT pair of subarrays. $L(L-1)/2$ different pairs of vector hydrophones may altogether be formed out of the L vector hydrophones. Each of these $L(L-1)/2$ ESPRIT vector-hydrophone pairs produces its own estimate of $\{\boldsymbol{a}(\theta_k,\phi_k), k=1,\cdots,K\}$, which must then be summed coherently to preserve signal power and to maximize noise cancellation.

Available at this point of the algorithm are the K number of $3L\times 1$ signal-subspace eigenvectors (10), from which the lth vector hydrophone's K number of 3×1 signal-subspace eigenvectors may be extracted as follows:

$$\boldsymbol{E}_l \stackrel{\text{def}}{=} (\boldsymbol{e}_l^H \otimes \boldsymbol{I}_3)\boldsymbol{E}_s, \quad \text{for} \quad l=1,\cdots,L \tag{15}$$

$$= [q_l(u_1,v_1)\boldsymbol{a}(\theta_1,\phi_1),\cdots,q_l(u_K,v_K)\boldsymbol{a}(\theta_K,\phi_K)]\boldsymbol{T} \tag{16}$$

$$\approx [\boldsymbol{a}(\theta_1,\phi_1),\cdots,\boldsymbol{a}(\theta_K,\phi_K)] \cdot \boldsymbol{Q}_l(u_1,\cdots,u_K,v_1,\cdots,v_K)\boldsymbol{T} \tag{17}$$

$$\boldsymbol{Q}_l(u_1,\cdots,u_K,v_1,\cdots,v_K) \stackrel{\text{def}}{=} \begin{bmatrix} q_l(u_1,v_1) & & 0 \\ & \ddots & \\ 0 & & q_l(u_K,v_K) \end{bmatrix} \tag{18}$$

where $\boldsymbol{e}_l$ denotes an $L\times 1$ vector with all zeros except a 1 in the lth position and $\boldsymbol{I}_3$ symbolizes a 3×3 identical matrix.

An ESPRIT matrix pencil pair involving the ith and the jth vector hydrophone may be formed using the two $3\times K$ matrices $\boldsymbol{E}_i$ and $\boldsymbol{E}_j$, which (being full rank) are related by a $K\times K$ nonsingular matrix $\boldsymbol{\Psi}_{ij}$:

$$\boldsymbol{E}_i\boldsymbol{\Psi}_{ij} = \boldsymbol{E}_j \tag{19}$$

$$\begin{aligned} \Rightarrow \boldsymbol{\Psi}_{ij} &= \left(\boldsymbol{E}_i^H\boldsymbol{E}_i\right)^{-1}\left(\boldsymbol{E}_i^H\boldsymbol{E}_j\right) \\ &= \boldsymbol{T}_{ij}^{-1}\boldsymbol{\Phi}_{ij}\boldsymbol{T}_{ij} \\ &= (\boldsymbol{P}_{ij}\boldsymbol{T}_{ij})^{-1}\tilde{\boldsymbol{\Phi}}_{ij}(\boldsymbol{P}_{ij}\boldsymbol{T}_{ij}) \end{aligned} \tag{20}$$

where $\boldsymbol{P}_{ij}$ symbolizes a $K\times K$ permutation matrix, $\boldsymbol{\Phi}_{ij}$ embodies a diagonal matrix whose diagonal element $[\boldsymbol{\Phi}_{ij}]_{kk}$ equals the eigenvalue of $\boldsymbol{\Psi}_{ij}$ with the corresponding eigenvector equal to the kth column of $\boldsymbol{T}_{ij}^{-1}$, the estimate of $\boldsymbol{T}$ in (17) using data from the ith and the jth vector hydrophones. $\tilde{\boldsymbol{\Phi}}_{ij}$ equals $\boldsymbol{\Phi}_{ij}$ except the diagonal elements are reordered. However, the above eigen-decomposition of $\boldsymbol{\Psi}_{ij}$ can only determine $\boldsymbol{T}_{ij}$ to within some column permutation. This is because (20) still holds replacing $\boldsymbol{T}_{ij}$ and $\boldsymbol{\Phi}_{ij}$, respectively, by $\boldsymbol{P}_{ij}\boldsymbol{T}_{ij}$ and $\boldsymbol{P}_{ij}\boldsymbol{\Phi}_{ij}(\boldsymbol{P}_{ij})^{-1}$. Under noiseless or asymptotic conditions (i.e., infinite number of data time samples),

$$\begin{aligned}[]&[\boldsymbol{a}(\theta_1, \phi_1, \gamma_1, \eta_1), \cdots, \boldsymbol{a}(\theta_K, \phi_K, \gamma_K, \eta_K)]\\ &\quad\cdot \boldsymbol{Q}_i(u_1, \cdots, u_K, v_1, \cdots, v_K)\boldsymbol{T}\boldsymbol{\Psi}_{ij}\\ &\quad= [\boldsymbol{a}(\theta_1, \phi_1, \gamma_1, \eta_1), \cdots, \boldsymbol{a}(\theta_K, \phi_K, \gamma_K, \eta_K)]\\ &\quad\cdot \boldsymbol{Q}_j(u_1, \cdots, u_K, v_1, \cdots, v_K)\boldsymbol{T} \end{aligned} \tag{21}$$

and $\boldsymbol{\Phi}_{ij} = \boldsymbol{Q}_i^{-1}\boldsymbol{Q}_j$. Note that ESPRIT may be concurrently applied to these $L(L-1)/2$ matrix pencil pairs by parallel computation.

In order to sum these $L(L-1)/2$ estimates of the K three-component velocity fields, the permutational ambiguities associated with $\{\boldsymbol{P}_{ij}, 1 \geq i < j \geq L\}$ must next be resolved. That is, $\boldsymbol{P}_{ij}$ must be estimated. Recognizing that $\boldsymbol{P}_{ij}\boldsymbol{T}_{ij}$ embodies a unitary matrix, the rows of $\boldsymbol{P}_{ij}\boldsymbol{T}_{ij}$ constitute an orthogonal set. Let l_k denotes the row-index of the matrix element with the largest absolute value in the kth column of the $K \times K$ matrix $(\boldsymbol{P}_{mn}\boldsymbol{T}_{mn})(\boldsymbol{P}_{ij}\boldsymbol{T}_{ij})^{-1}$. Then the l_kth row of $\boldsymbol{P}_{mn}\boldsymbol{T}_{mn}$ must correspond to the lth row of $\boldsymbol{P}_{ij}\boldsymbol{T}_{ij}$. This permutation procedure requires *no* exhaustive searches and thus requires minimum computation.

Having thus permuted $\{\boldsymbol{P}_{ij}\boldsymbol{T}_{ij}, 1 \leq i < j \leq L\}$ to obtain $\{\boldsymbol{T}_{ij}, 1 \leq i < j \leq L\}$, $\{\boldsymbol{E}_l, 1 \leq l \leq L\}$ may now be decoupled and coherently summed to yield a composite estimate $\hat{\boldsymbol{a}}_k$ of the K velocity fields $\{\boldsymbol{a}(\theta_k, \phi_k), k = 1, \cdots, K\}$

$$\hat{\boldsymbol{a}}_k = \frac{\left[\displaystyle\sum_{1<i<j\leq L} \left(\boldsymbol{E}_i\boldsymbol{T}_{ij}^{-1} + \boldsymbol{E}_j\boldsymbol{T}_{ij}^{-1}\boldsymbol{\Phi}_{ij}\right)\boldsymbol{\Phi}_{1i}\right]\boldsymbol{e}_k}{\left\|\left[\displaystyle\sum_{1\leq i<j\leq L} \left(\boldsymbol{E}_i\boldsymbol{T}_{ij}^{-1} + \boldsymbol{E}_j\boldsymbol{T}_{ij}^{-1}\boldsymbol{\Phi}_{ij}\right)\boldsymbol{\Phi}_{1i}\right]\boldsymbol{e}_k\right\|} \tag{22}$$

where $\boldsymbol{\Phi}_{11} \stackrel{\text{def}}{=} \boldsymbol{I}_2$. $\boldsymbol{\Phi}_{ij}$ renders the summation of $\boldsymbol{E}_i\boldsymbol{T}_{ij}^{-1}$ and $\boldsymbol{E}_j\boldsymbol{T}_{ij}^{-1}$ coherent for any particular i and j. Similarly, $\boldsymbol{\Phi}_{1i}$ renders the summation of $\{\boldsymbol{E}_i\boldsymbol{T}_{ij}^{-1} + \boldsymbol{E}_j\boldsymbol{T}_{ij}^{-1}\boldsymbol{\Phi}_{ij}, i = 1, \cdots, L\}$ coherent. The computation of all $L(L-1)/2$ matrix pencil pairs maximizes noise cancellation because it utilizes data collected from all L vector hydrophones and exploits all spatial invariances among all L vector hydrophones. However, it may be possible to economize on computation by performing TLS-ESPRIT on only a subset of all $L(L-1)/2$ possible pairs. The drawback of not computing all $L(L-1)/2$ pairs is a less optimum decoupling of the sources' steering vector, resulting in less accurate coarse DOA estimates (to be derived below) and less effective source selectivity in the LCMV beamforming.

As a side note, many of these $L(L-1)/2$ ESPRIT vector-hydrophone pairs may possess an intervector-hydrophone spacing in excess of a half wavelength. This will result in a cyclic ambiguity of some integer multiple of 2π in ESPRIT's eigenvalues' phases. The one-to-one mapping between ESPRIT's eigenvalues' phase angles and the direction-cosines will thus no longer exist, and no unambiguous direction-cosine estimates may be obtainable from ESPRIT's eigenvalues. However, given that it is $\boldsymbol{T}$, not ESPRIT's eigenvalues, that is needed in the algorithm, this cyclic ambiguity of ESPRIT's eigenvalues' phases is irrelevant to the objective at hand. TLS-ESPRIT, regardless of the intervector-hydrophone spacing, can always estimate $\boldsymbol{T}_{ij}$ and $\boldsymbol{\Psi}_{ij}$, and these are all that matter here. In other words, initial coarse estimates of the direction-cosines are derived not from ESPRIT's eigenvalues, as is often the case, but from ESPRIT's signal-subspace eigenvectors. In contrast, ESPRIT's signal-subspace eigenvectors are usable here because they do not suffer any ambiguity due to extended intervector-hydrophone spacing. For the vector hydrophone, knowledge of these signal-subspace eigenvectors leads to direct estimation (via the normalization estimator) of the direction-cosines due to the unique form of the vector hydrophone's manifold. If each vector hydrophone is replaced by a subarray of displaced pressure hydrophones, then the present algorithm would not work because there is no simple way to extract the direction-cosine information from the subarray manifold of a subarray of displaced pressure hydrophones without performing another MUSIC-like search over the subarray manifold.

D. Self-Initiating MUSIC-Based DF in Acoustic Particle Velocity-Field Beamspace

Applying MUSIC to the LCMV acoustic particle velocity-field beamformer output, the direction-cosine estimates for the kth source are

$$\{\hat{u}_k, \hat{v}_k\} \stackrel{\text{def}}{=} \underset{u,\,v}{\arg\max}\, \|\boldsymbol{E}_{b_k}^H \boldsymbol{q}(u, v)\|. \tag{23}$$

Note that, unlike customary formulation of the MUSIC algorithm, the kth source's signal-subspace steering vector, not the null-space eigenvectors, is used in the above optimization. It is preferable here to use $\boldsymbol{E}_{b_k}$ rather than the null-space eigenvectors because the latter, being orthogonal to all $\{\boldsymbol{q}(u_k, v_k), k = 1, \cdots, K\}$, contain "contaminating" information from the spatial phase factors of all the other K sources. In contrast, $\boldsymbol{E}_{b_k}$, as the output of the LCMV beamformer nulling out all signals other than the kth signal, contains information only of the kth source. Thus, using $\boldsymbol{E}_{b_k}$ in (23) removes spectral optima corresponding to the interferers, resulting in a "flattened" scalar function for optimization and thus yielding faster convergence to more accurate arrival angle estimates. As a side note, customary formulations of MUSIC use the null-space eigenvectors and not the signals' steering vectors in the above optimization also because the individual sources' steering vectors are unavailable. The signal-subspace eigenvector set (i.e., the columns of $\boldsymbol{E}_s$) cannot ordinarily be decoupled into the K impinging sources' respective steering vectors. In contrast, this decoupling can be successfully performed using techniques described in the preceding subsections. Thus, the MUSIC-based search of this algorithm can use each individual source's steering vector estimate instead of the null-space eigenvectors.

A set of coarse direction-cosine estimates $\{\hat{u}_k^{\text{coar}}, \hat{v}_k^{\text{coar}}, \hat{w}_k^{\text{coar}}\}$ may be obtained to initiate the iterative search in (23) by normalizing each signals' steering vector estimate

$$\begin{bmatrix} \hat{u}_k^{coar} \\ \hat{v}_k^{coar} \\ \hat{w}_k^{coar} \end{bmatrix} = \frac{\hat{\boldsymbol{a}}_k}{\mathrm{sgn}([\hat{\boldsymbol{a}}_k]_3)}$$

where

$$\mathrm{sgn}(x) \stackrel{\mathrm{def}}{=} \begin{cases} 1 & \text{if } x \geq 0 \\ -1 & \text{if } x < 0 \end{cases}. \tag{24}$$

$\mathrm{sgn}([\hat{\boldsymbol{a}}_k]_3)$ is used above because the sources are assumed to locate in the upper hemisphere. From the direction-cosine estimates derived in (23), the kth signal's azimuth and elevation arrival angles can be estimated as

$$\hat{\theta}_k = \sin^{-1}\sqrt{\hat{u}_k^2 + \hat{v}_k^2} = \cos^{-1}\hat{w}_k \tag{25}$$

$$\hat{\phi}_k = \tan^{-1}\frac{\hat{v}_k}{\hat{u}_k}. \tag{26}$$

Note that these estimates of the sources' azimuth angles and elevation angles have already been automatically matched with no additional processing.

E. Alternative Constructions of the Vector Hydrophone

1) Alternate Construction #1: It is possible to add an extra pressure hydrophone in spatial co-location to the existing velocity-hydrophone triad subarray unit. Acoustic particle motion sensors, by themselves, suffer a 180° ambiguity, with their plane-wave response given by the "figure 8" curve. However, the addition of a pressure hydrophone breaks this ambiguity because a hydrophone distinguishes between acoustical compressions and dilations. This new setup expands the 3×1 array manifold in (1) to a 4×1 array manifold [16]

$$\boldsymbol{a}(\theta_k, \phi_k) \stackrel{\mathrm{def}}{=} \begin{bmatrix} 1 \\ \sin\theta_k \cos\phi_k \\ \sin\theta_k \sin\phi_k \\ \cos\theta_k \end{bmatrix}. \tag{27}$$

All other equations in the previous exposition are to be similarly expanded in a straightforward fashion. With this four-component vector-hydrophone construction, sources may be located to either side of the array, that is, θ_k may range in $0 \leq \theta_k < \pi$ instead of $0 \leq \theta_k < \pi/2$. The number of resolvable sources is increased to three (the following section will discuss how to increase to an arbitrarily large number of resolvable sources).

This additional pressure hydrophone also allows additional noise cancellation using the Lagrange multiplier method to harmonize the two separate measurements, $[\hat{\boldsymbol{a}}_k]_1$ and $\sqrt{\{([\hat{\boldsymbol{a}}_k]_2)^2 + ([\hat{\boldsymbol{a}}_k]_3)^2 + ([\hat{\boldsymbol{a}}_k]_4)^2\}}$, of the normalized pressure. That is, an optimal set of perturbation weights $\{w_{1_k}, w_{2_k}, w_{3_k}, w_{4_k}\}$ relating the elements of $\hat{\boldsymbol{a}}_k$

$$(1 + w_{1_k})([\hat{\boldsymbol{a}}(\theta_k, \phi_k)]_1)^2 = \Sigma_{l=2}^4 (1 + w_{l_k})([\hat{\boldsymbol{a}}(\theta_k, \phi_k)]_l)^2 \tag{28}$$

may be derived to harmonize these two entities as follows. Recasting this objective in the theoretical framework of an optimization problem:, $w_{1_k}^2 + w_{2_k}^2 + w_{3_k}^2 + w_{4_k}^2$ is to be minimized given the constraint in (28). The optimal perturbation weights are then

$$w_{2_k} = -\frac{\lambda}{2}[\hat{\boldsymbol{a}}_k]_2 \tag{29}$$

$$w_{3_k} = -\frac{\lambda}{2}[\hat{\boldsymbol{a}}_k]_3 \tag{30}$$

$$w_{4_k} = -\frac{\lambda}{2}[\hat{\boldsymbol{a}}_k]_4 \tag{31}$$

$$\lambda = 2\frac{\sum_{l=2}^{4}([\hat{\boldsymbol{a}}_k]_l)^2 - ([\hat{\boldsymbol{a}}_k]_1)^2}{\sum_{l=2}^{4}([\hat{\boldsymbol{a}}_k]_l)^4 - ([\hat{\boldsymbol{a}}_k]_1)^4}. \tag{32}$$

Thus, the improved coarse reference direction-cosine estimates are

$$\hat{u}_k \stackrel{\mathrm{def}}{=} \sqrt{1 + w_{2_k}}[\hat{\boldsymbol{a}}_k]_2 \tag{33}$$

$$\hat{v}_k \stackrel{\mathrm{def}}{=} \sqrt{1 + w_{3_k}}[\hat{\boldsymbol{a}}_k]_3 \tag{34}$$

$$\hat{w}_k \stackrel{\mathrm{def}}{=} \sqrt{1 + w_{4_k}}[\hat{\boldsymbol{a}}_k]_4. \tag{35}$$

2) Alternate Construction #2: The underwater acoustic velocity field may be characterized by its three Cartesian components, or it may alternately be characterized by its two components along the x axis and the y axis plus the overall pressure field. A vector hydrophone comprising only the two horizontally oriented velocity hydrophones plus a pressure hydrophone can avoid directly dealing with the vertical component of the underwater acoustical particle motion. This constitutes an important consideration because particle motion may be circularly and elliptically polarized and need not be rectilinear. Even if the source initially generates a single plane-wave, the multipath propagation properties of the ocean environment typically lead to elliptically polarized particle motion. By eliminating the vertical velocity hydrophone, the mathematical data model presented in the preceding sections will better model actual ocean acoustics. In this case, the sources would be presumed to be impinging from only one side of the array plane. Then, the vector-hydrophone array manifold in (1) becomes

$$\boldsymbol{a}_k = \begin{bmatrix} \sin\theta_k \cos\phi_k \\ \sin\theta_k \sin\phi_k \\ 1 \end{bmatrix}. \tag{36}$$

The kth source's coarse but unambiguous direction-cosine estimates may then be obtained from $\hat{\boldsymbol{a}}_k$ of (1) as follows

$$\hat{u}_k = [\hat{\boldsymbol{a}}_k]_1/[\hat{\boldsymbol{a}}_k]_3 \tag{37}$$

$$\hat{v}_k = [\hat{\boldsymbol{a}}_k]_2/[\hat{\boldsymbol{a}}_k]_3 \tag{38}$$

$$\hat{w}_k = \sqrt{1 - \hat{u}_k^2 - \hat{v}_k^2}. \tag{39}$$

However, it would always be necessary to have at least three co-located hydrophones in each vector-hydrophone unit so as to have sufficient information to obtain properly normalized direction-cosine estimates.

F. Extension to Irregularly Spaced Subarrays of Vector Hydrophones

This section presents an extension to accommodate more than the two-source maximum permitted by the basic algorithm presented in the preceding subsections. This two-source constraint arises from the 3×1 size of the vector-hydrophone's array manifold. This maximum may readily be raised to $3\tilde{L}-1$ or $3L-1$ by replacing each of the L irregularly spaced vector hydrophones with a subarray of $\tilde{L}$ vector hydrophones. Such subarrays of $\tilde{L}$ vector hydrophones may have an irregular configuration so long as one identical subarray configuration is used.

The overall $3L\tilde{L}\times 1$ array manifold for the kth incident source becomes

$$\boldsymbol{a}(\theta_k, \phi_k) \stackrel{\text{def}}{=} \boldsymbol{q}(u_k, v_k) \otimes \begin{bmatrix} q_1^{\text{sub}}(u_k, v_k) \\ \vdots \\ q_{\tilde{L}}^{\text{sub}}(u_k, v_k) \end{bmatrix} \otimes \begin{bmatrix} u(\theta_k, \phi_k) \\ v(\theta_k, \phi_k) \\ w(\theta_k) \end{bmatrix} \tag{40}$$

$$q_m^{\text{sub}}(u_k, v_k) \stackrel{\text{def}}{=} \exp\left(j2\pi \frac{x_m^{\text{sub}} u_k + y_m^{\text{sub}} v_k + z_m^{\text{sub}} w_k}{\lambda} \right) \tag{41}$$

where $(x_m^{\text{sub}}, y_m^{\text{sub}}, z_m^{\text{sub}})$ denotes the location of the subarray's mth vector hydrophone *relative* to the subarray's first vector hydrophone located at $(x_1^{\text{sub}}, y_1^{\text{sub}}, z_1^{\text{sub}})$.

Previous algorithmic developments in Section III and all equations (1)–(25) still hold with the following changes: $\boldsymbol{a}(\theta_k, \phi_k)$, $\boldsymbol{a}_l(\theta_k, \phi_k)$, $\boldsymbol{z}_l(t)$, $\boldsymbol{w}_k$, and $\hat{\boldsymbol{a}}_l(\theta_k, \phi_k)$ become $3\tilde{L} \times 1$ in size; $\boldsymbol{z}(t)$ and $\boldsymbol{n}(t)$ both become $3L\tilde{L} \times 1$; $\boldsymbol{A}$, $\boldsymbol{E}_s$, and $\boldsymbol{C}$ become $3L\tilde{L} \times K$; $\boldsymbol{z}_l$ becomes $3\tilde{L} \times N$, $\boldsymbol{Z}$ becomes $3L\tilde{L} \times N$; $\hat{\boldsymbol{R}}_{zz}$ becomes $3L\tilde{L} \times 3L\tilde{L}$, while $\boldsymbol{R}_{vh}$ becomes $3\tilde{L} \times 3\tilde{L}$. Equation (15) also becomes

$$\boldsymbol{E}_l = \left(\boldsymbol{e}_l^H \otimes \boldsymbol{I}_{3\tilde{L}} \right) \boldsymbol{E}_s \tag{42}$$

where $\boldsymbol{e}_l$ refers to an $L \times 1$ vector with all zeros except a 1 at the lth position. $\boldsymbol{e}_l$ selects the sector of $\boldsymbol{E}_s$ corresponding to the lth subarray and stores that information in $\boldsymbol{E}_l$. Also, (22) now produces the $3\tilde{L} \times 1$ subarray manifold estimates, from which the kth source's three velocity-field components may be derived as follows:

$$\hat{\boldsymbol{p}}_k = \frac{\Sigma_{\tilde{l}=1}^{\tilde{L}} (\boldsymbol{I}_3 \otimes \boldsymbol{e}_l^T) \hat{\boldsymbol{a}}_k}{||\Sigma_{\tilde{l}=1}^{\tilde{L}} (\boldsymbol{I}_3 \otimes \boldsymbol{e}_l^T) \hat{\boldsymbol{a}}_k||} \tag{43}$$

where $\boldsymbol{e}_l$ is now an $\tilde{L} \times 1$ vector. $\hat{\boldsymbol{p}}_k$ produces initial direction-cosine estimates for MUSIC's iterative search. Equation (14) also becomes

$$\boldsymbol{E}_{b_k} \stackrel{\text{def}}{=} (\boldsymbol{I}_L \otimes \boldsymbol{w}_k^H) \boldsymbol{E}_s \tag{44}$$

where $\mathbf{1}^{\tilde{L}}$ denotes a $1 \times \tilde{L}$ vector of ones. These modifications permit the proposed method to handle up to $3\tilde{L} - 1$ sources. If $L > \tilde{L}$, then more sources can be accommodated if the above array configuration of $L\tilde{L}$ vector hydrophones is viewed as $\tilde{L}$ identical but translated subarrays of L irregularly spaced vector hydrophones. In this case, up to $3L-1$ sources may be handled.

IV. Simulations

Simulation results in Figs. 1–4 verify the efficacy of the proposed self-initiating MUSIC-based DF algorithm. For all these figures, there exist two closely spaced equal-power uncorrelated narrow-band incident sources with the following parameters: $\theta_1 = 58.07°$, $\phi_1 = 44.05°$, $\theta_2 = 59.10°$, and $\phi_2 = 36.47°$. That is, the signal-of-interest (with subscript 1) has $u_1 = 0.61$ and $v_1 = 0.59$ and the interference (with subscript 2) has $u_2 = 0.69$ and $v_2 = 0.51$. To simulate the proposed self-initiating velocity-field beamspace vector-hydrophone MUSIC algorithm, 13 identically oriented vector hydrophones (each composed of three orthogonally oriented velocity hydrophones) are used at the (x, y, z) coordinates:

$$\frac{7\lambda}{2} \times \{(0, 0, 0), (\pm 1, 0, 0)(\pm 2.7, 0, 0), (0, \pm 1, 0), (0, \pm 2.7, 0), (\pm 4.1, -4.1, 1), (\pm 4.1, 4.1, -1)\}$$

where λ denotes the sources' common wavelength. Neither ESPRIT nor Root-MUSIC can effectively process all data sets collected from all sensors constituting such an irregularly spaced array. Only $L - 1 = 12$ TLS-ESPRIT matrix pencil pairs—those involving the $(0, 0, 0)$ vector hydrophone and one of the other 12—have been processed to estimate the three velocity-field components in (22). The acoustic particle velocity-field LCMV beamformer in (14) is set to pass only the first source and to null the second source. The additive white noise is complex Gaussian, and the SNR is defined relative to each source. One hundred snapshots are used in each of the 500 independent Monte Carlo simulation experiments. The estimation error in each experiment is computed by finding the difference between $\{\hat{u}, \hat{v}\}$ and the direction-cosines of whichever source is closest to the estimated direction-cosines (to be discussed more fully below). The Nelder–Meade simplex algorithm is used in the iterative searches.

Figs. 1 and 2, respectively, plot the direction-cosines' composite estimation standard deviation and bias at different SNR's for the proposed algorithm. The composite rms standard deviation equals the square root of the mean of the respective sample variances of $\hat{u}$ and $\hat{v}$; the composite bias equals the square root of the mean of the square of the respective sample biases of $\hat{u}$ and $\hat{v}$. The estimation standard deviation is close to the Cramer–Rao lower bound for an SNR above 5 dB. Because $u_2 - u_1 = v_1 - v_2 = 0.08$, the two sources would be resolved and identified with high probability if both the estimation standard deviation and the bias are under approximately 0.03. Referring to these two figures, the proposed blind algorithm successfully resolved these closely-spaced sources for all SNR's above 0 dB without any *a priori* information on the sources' directions of arrival.

Very occasionally, the iterative search proposed in Section III converges to the spectral optimum corresponding to the nulled source rather than to the passed source. The frequency of this misconvergence to the nulled source is plotted in Fig. 3. Note

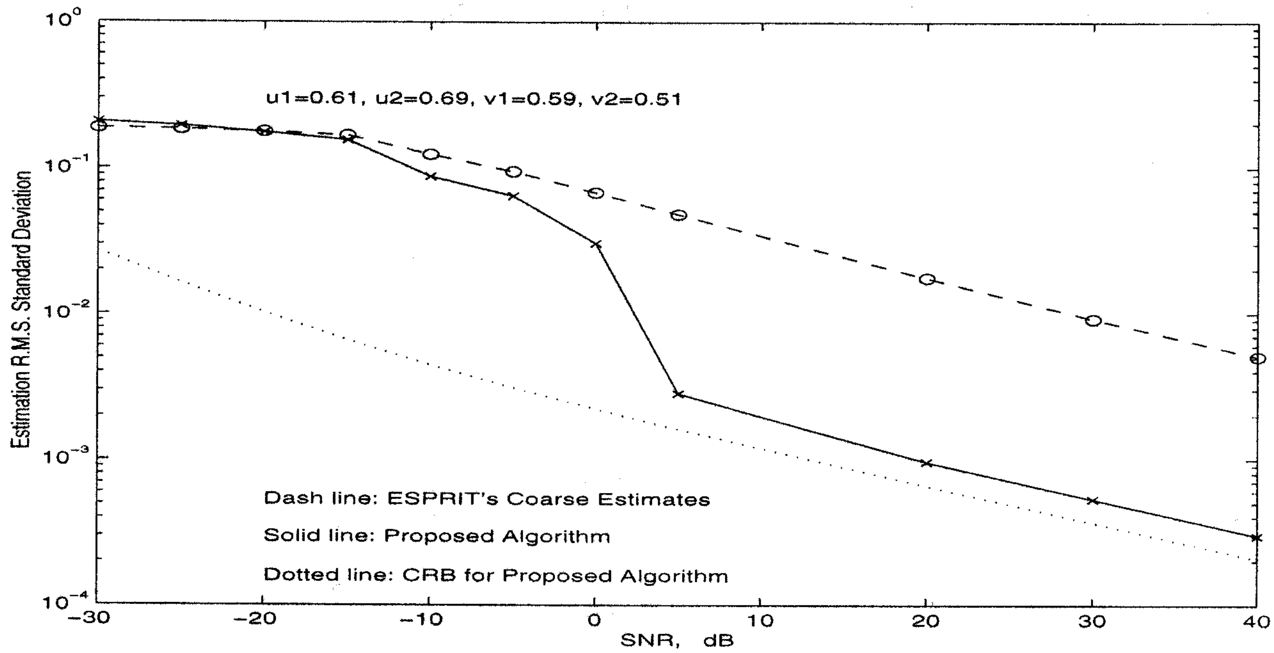

Fig. 1. RMS standard deviation of $\{\hat{u}_1, \hat{v}_1\}$ versus SNR: two closely-spaced equal-power uncorrelated narrow-band incident sources with $\theta_1 = 58.07°$, $\phi_1 = 44.05°$, $\mathcal{P}_1 = 1$, $\theta_2 = 59.10°$, $\phi_2 = 36.47°$, $\mathcal{P}_2 = 1$, 100 snapshots per experiment, and 500 independent experiments per data point.

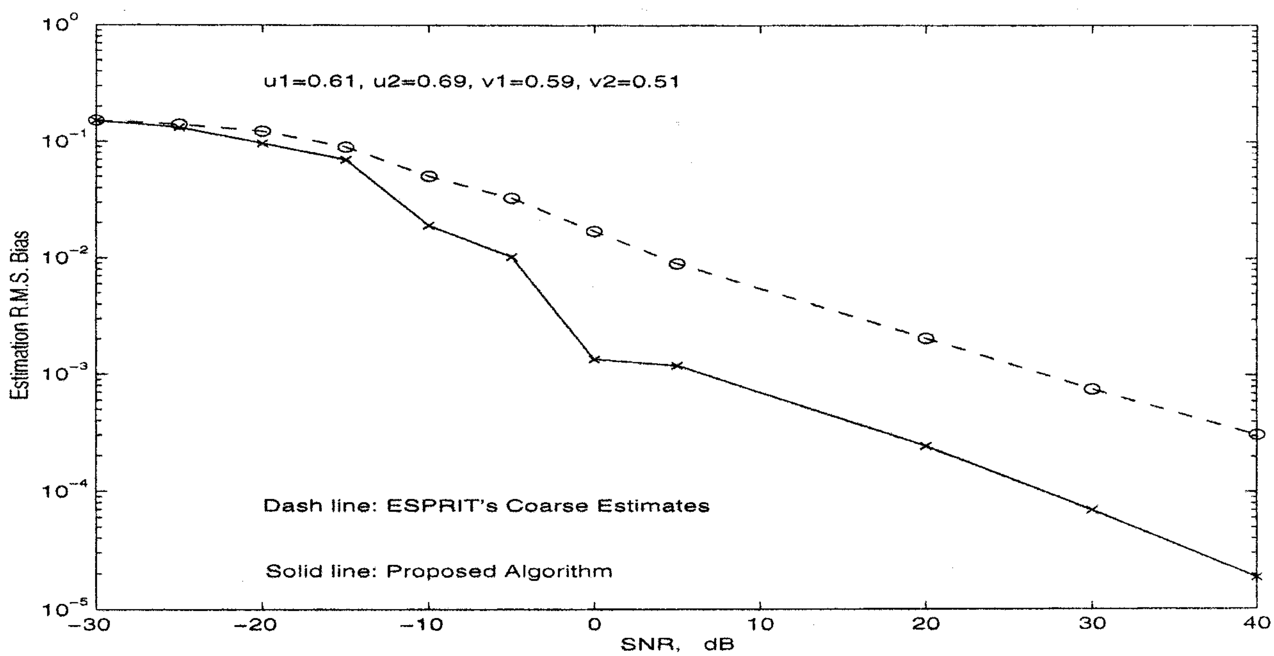

Fig. 2. RMS bias of $\{\hat{u}_1, \hat{v}_1\}$ versus SNR: the same settings as in Fig. 1.

that at high SNR's at or above 20 dB, misconvergence does not occur at all. As the SNR becomes more demanding, misconvergence gradually increases. This phenomenon of misconvergence to the supposedly nulled source may be explained by the imperfect decoupling of the signal-subspace eigenvectors into the sources' individual array manifolds in (22) as noise intensity increases. Thus, the LCMV beamformer fails to block out the phase-delay spectrum of the supposedly nulled source, and the iterative search misconverges to the direction-cosines of this source. This problem may be minimized by computing more TLS-ESPRIT matrix pencil pairs (instead of only $L-1$ pairs as performed for these simulation results) in (22) to obtain better decoupling of the signal-subspace eigenvectors. Convergence behavior of the MUSIC-based iterative search is integrally connected with the particular search algorithm used. MATLAB's built-in function "fmins" utilized for these simulations uses the Nelder–Meade simplex algorithm. A more sophisticated search algorithm could well offer better converge results. In any case, this misconvergence to an unintended source need not be a problem if, in each velocity-beam space iterative search, K optima (instead of just one optimum) are to be determined.

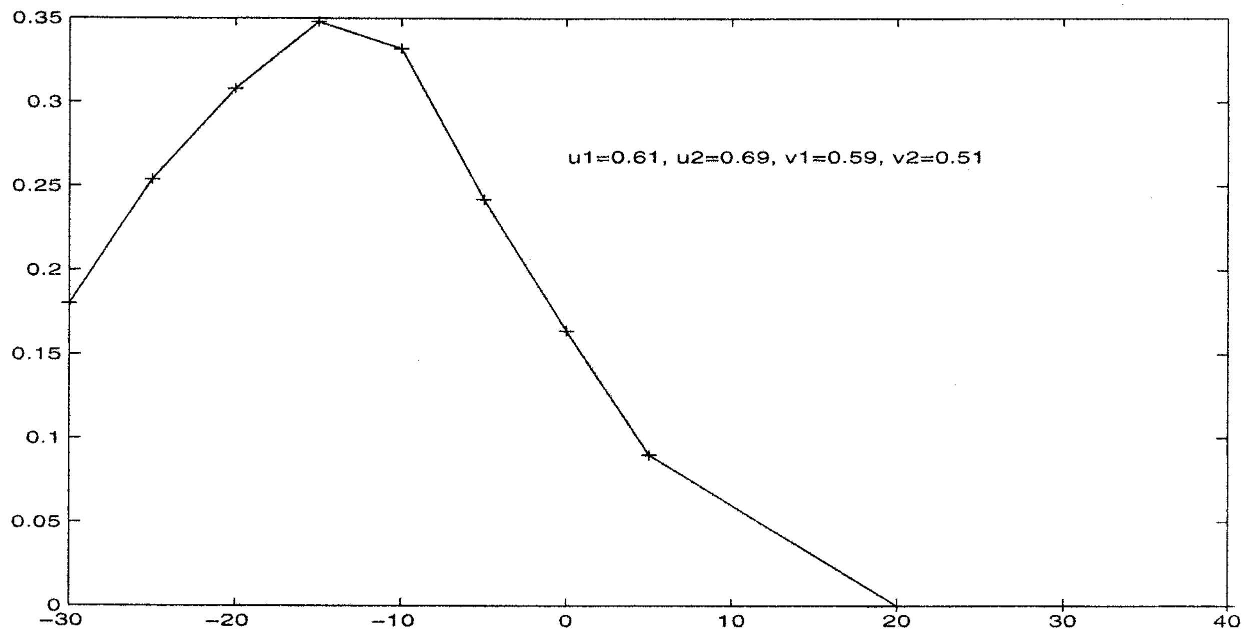

Fig. 3. Fraction of misconvergence to "nulled" source versus SNR: the same settings as in Fig. 1.

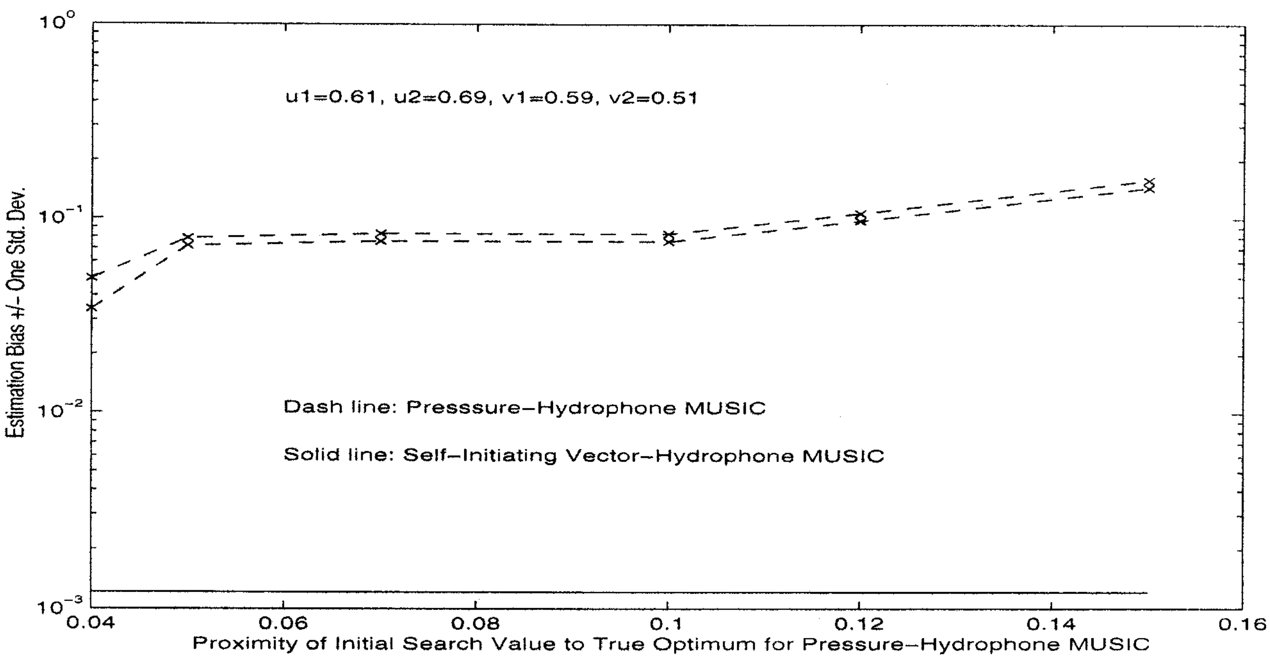

Fig. 4. RMS error of $\{\hat{u}_1, \hat{v}_1\}$ versus proximity of the initial estimate $\{u_1^\circ, v_1^\circ\}$ to the true values. The same settings as in Fig. 1.

Fig. 4 demonstrates the advantage offered by the proposed algorithm's self-initiating capability by comparing the estimation errors of the proposed algorithm with the estimation errors of customary MUSIC applied to a comparable pressure-hydrophone array and supplied with a close initial search value. This customary pressure-hydrophone MUSIC algorithm is simulated for 39 pressure hydrophones grouped into 13 three-element subarrays, with each subarray having an L-shaped configuration $\lambda/2\{(0, 0, 0), (1, 0, 0), (0, 1, 0)\}$. These 13 subarrays are located in an identical configuration as the aforementioned 13-vector-hydrophone array. Note that this 39-pressure-hydrophone array possesses an identical number of hydrophones as the 13-vector-hydrophone array and that these two arrays have nearly the same physical aperture. The simulation scenario here is identical to that for Figs. 1–3, except the SNR is constant at 10 dB and the proximity of the available initial search direction-cosine estimates to the true direction-cosine values for pressure-hydrophone MUSIC is varied. The two parallel lines with x's in Fig. 4 give the performance of the 39-pressure-hydrophone array in terms of estimation bias $\pm$ one estimation standard deviation. The solid line shows the estimation bias plus one estimation standard deviation for the proposed algorithm. The estimation bias is negligible relative to the estimation standard deviation for the vector-hydrophone case, because the proposed self-initiating algorithm needs no *a priori* coarse initial search value. In contrast, bias dominates standard deviation for the pressure-hydrophone array because the optimization here converges to a local optimum, instead of the true global optimum. Note that, even when the supplied initial search value is within 0.04 of the signal's direction cosines, customary pressure-hydrophone MUSIC still under-performs (due to misconvergence to a wrong local optimum) relative to the proposed self-initiating acoustic particle velocity-field MUSIC method.

V. Conclusions

This novel self-initiating MUSIC-based DF algorithm in underwater acoustic particle velocity-field beamspace utilizes vector hydrophones instead of pressure hydrophones. The recognition of the impinging underwater acoustic wavefield as a vector field instead of a mere intensity field allows DF by normalizing the the vector-hydrophone steering vectors, rather than through estimating inter-element spatial phase delays as is customarily done. The underwater acoustic particle velocity-field beamformer reduces the complexity of the scalar function to be searched and removes false optima due to interferers. The normalization estimator further supplies coarse direction-cosine estimates to start off the velocity-field beamspace MUSIC's iterative search over the intervector-hydrophone spatial phase-delay array manifold *without* any *a priori* information on the sources' parameters, thereby facilitating *faster* convergence to the *global* optimum. Simulation results verify the efficacy of this blind beamforming and DF algorithm. While the preceding algorithmic development has assumed that all L vector hydrophones are identically oriented, a simple correctional procedure is presented in [25] to accommodate any nonidentical orientation among the L vector hydrophones. Though the incident signals have been assumed to be narrow-band, broad-band signals may be readily handled by reducing the broad-band problem to a set of narrow-band problems via the use of a comb of narrow-band filters. Furthermore, even though this algorithm is in the batch processing mode, its real-time adaptive implementation for nonstationary environments may be readily implemented using fast recursive eigen-decomposition updating methods such as those in [15] and [17]. An electromagnetic analog of the proposed scheme is available in [26].

Acknowledgment

The authors would like to thank the anonymous reviewers for many helpful suggestions. The manuscript has significantly improved as a result.

References

[1] C. B. Leslie, J. M. Kendall, and J. L. Jones, "Hydrophone for measuring particle velocity," *J. Acoust. Soc. Amer.*, vol. 28, no. 4, pp. 711–715, July 1956.

[2] O. L. Frost, "An algorithm for linearly constrained adaptive array processing," *Proc. IEEE*, vol. 60, pp. 926–935, Aug. 1972.

[3] *Handbook of Hydrophone Element Design Technology*, Naval Underwater Systems Center, 1978.

[4] M. A. Josserand and C. Maerfeld, "PVF2 velocity hydrophone," *J. Acoust. Soc. Amer.*, vol. 78, no. 3, pp. 860–867, 1985.

[5] R. O. Schmidt, "Multiple emitter location and signal parameter estimation," *IEEE Trans. Antennas Propagat.*, vol. AP-34, pp. 276–280, March 1986.

[6] V. J. Hughes, J. G. Boulton, J. M. Coles, T. R. Empson, and N. J. Kerry, "Why an optically-based hydrophone works better," *Sensor Review*, vol. 7, no. 3, pp. 123–126, Jul. 1987.

[7] R. Roy and T. Kailath, "ESPRIT-estimation of signal parameters via rotational invariance techniques," *IEEE Trans. Acoustics, Speech, Signal Processing*, vol. 37, pp. 984–995, Jul. 1989.

[8] X. Xu and K. Buckley, "Statistical performance comparison of MUSIC in element-space and beam-space," in *IEEE ICASSP*, 1989, pp. 2124–2127.

[9] H. Lee and M. Wengrovitz, "Resolution threshold of beamspace MUSIC for two closely spaced emitters," *IEEE Trans. Acoustics, Speech, Signal Processing*, vol. 38, pp. 1545–1559, Sept 1990.

[10] P. Stoica and A. Nehorai, "Comparative performance study of element-space and beam-space MUSIC estimators," *Circuits, Systems, & Signal Processing*, vol. 10, no. 3, pp. 285–292, 1991.

[11] G. L. D'Spain, W. S. Hodgkiss, and G. L. Edmonds, "The simultaneous measurement of infrasonic acoustic particle velocity and acoustic pressure in the ocean by freely drifting swallow floats," *IEEE J. Oceanic Eng.*, vol. 16, pp. 195–207, 1991.

[12] J. C. Nickles, G. Edmonds, R. Harriss, F. Fisher, W. S. Hodgkiss, J. Giles, and G. D'Spain *et al.*, "A vertical array of directional acoustic sensors," in *IEEE Oceans 92 Conf.*, pp. 340–345.

[13] G. L. D'Spain, W. S. Hodgkiss, G. L. Edmonds, J. C. Nickles, F. H. Fisher, and R. A. Harris *et al.*, "Initial analysis of the data from the vertical DIFAR array," in *IEEE Oceans 92 Conf.*, pp. 346–351.

[14] V. A. Shchurov, V. I. Ilyichev, and V. P. Kuleshov, "Ambient noise energy motion in the near-surface layer in ocean wave-guide," *J. Phys.*, pt. 2, vol. 4, no. 5, pp. 1273–1276, May 1994.

[15] M. Moonen, F. J. Vanpoucke, and E. F. Deprettere, "Parallel and adaptive high-resolution direction finding," *IEEE Trans. Signal Processing*, vol. 42, pp. 2439–2448, Sept. 1994.

[16] A. Nehorai and E. Paldi, "Acoustic vector-sensor array processing," *IEEE Trans. Signal Processing*, vol. 42, pp. 2481–2491, Sep. 1994.

[17] B. Champagne, "Adaptive eigendecomposition of data covariance matrices based on first-order perturbations," *IEEE Trans. Signal Processing*, vol. 42, pp. 2758–2770, Oct. 1994.

[18] M. Hawkes and A. Nehorai, "Bearing estimation with acoustic vector-sensor arrays," in *Acoustic Velocity Focused Workshop*, 1995, pp. 345–348.

[19] M. Hawkes and A. Nehorai, "Hull-mounted acoustic vector-sensor arrays," in *29th Asilomar Conf.*, 1995.

[20] M. Hawkes and A. Nehorai, "Surface mounted acoustic vector-sensor array beamforming," in *IEEE Int. Conf. Acoustic, Speech & Signal Processing*, 1996, pp. 3170–3173.

[21] B. Hochwald and A. Nehorai, "Identifiability in array processing models with vector-sensor applications," *IEEE Trans. Signal Processing*, vol. 44, pp. 83–95, Jan. 1996.

[22] M. J. Berliner and J. F. Lindberg, *Acoustic Particle Velocity Sensors: Design, Performance and Applications*. Woodbury, NY: AIP Press, 1996.

[23] K. T. Wong and M. D. Zoltowski, "Orthogonal-velocity-hydrophone ESPRIT for sonar source localization," in *MTS/IEEE Oceans'96 Conf.*, pp. 1307–1312.

[24] ——, "Extended-aperture underwater acoustic multisource azimuth/elevation direction-finding using uniformly but sparsely spaced vector hydrophones," *IEEE J. Oceanic Eng.*, vol. 22, pp. 659–672, Oct. 1997.

[25] ——, "Closed-form underwater acoustic direction-finding with arbitrarily spaced vector hydrophones at unknown locations," *IEEE J. Oceanic Eng.*, vol. 22, pp. 566–575, July 1997.

[26] ——, "Polarization-beamspace self-initiating MUSIC for azimuth/elevation angle estimation," in *IEE Radar'97 Conf.*, pp. 328–333.

[27] ——, "Self-initiating velocity-field beamspace MUSIC for underwater acoustic direction-finding with irregularly spaced vector-hydrophones," in *IEEE Int. Symp. Circuits & Systems*, vol. 4, 1997, pp. 2553–2556.

[28] M. Hawkes and A. Nehorai, "Acoustic vector-sensor beamforming and capon direction estimation," *IEEE Trans. Signal Processing*, vol. 46, pp. 2291–2304, Sept. 1998.

[29] K. T. Wong and M. D. Zoltowski, "Root-MUSIC-based azimuth-elevation angle-of-arrival estimation with uniformly spaced but arbitrarily oriented velocity hydrophones," *IEEE Trans. Signal Processing*, vol. 47, pp. 3250–3260, Dec. 1999.

[30] K. T. Wong, "Adaptive source localization & blind beamforming for underwater acoustic wideband fast frequency-hop signals of unknown hop sequences & unknown arrival angles using a vector-hydrophone," in *IEEE Wireless Communications & Networking Conf.*, 1999.

[31] K. T. Wong and H. Chi, "Beam patterns of an underwater acoustic vector hydrophone," presented at the 2000 IEEE Signal Processing Workshop on Statistical Signal and Array Processing.

Kainam T. Wong (S'86–M'97) received the B.S.E. degree in chemical engineering from the University of California at Los Angeles in 1985, the B.S.E.E. degree from the University of Colorado, Boulder, in 1987, the M.S.E.E. degree from the Michigan State University, East Lansing, in 1990, and the Ph.D. degree in electrical engineering from Purdue University, West Lafayette, IN, in 1996.

He was a Manufacturing Engineer at the General Motors Technical Center, Warren, MI, from 1990 to 1991, a Senior Professional Staff Member at the Johns Hopkins University Applied Physics Laboratory, Laurel, MD, from 1996 to 1998, an Assistant Professor at Nanyang Technical University, Singapore, in 1998, and is presently an Assistant Professor in the Department of Electronic Engineering, Chinese University of Hong Kong, since August 1998. He is a contributing author of approximately 70 articles for the telecommunications section of the inaugural edition of the *CRC Dictionary of Pure & Applied Physics* and the *CRC Comprehensive Dictionary of Physics*. His research interests are sensor array signal processing and signal processing for communications.

Dr. Wong has served on the Technical Program Committees of the 1999 and 2000 IEEE Wireless Communications and Networking Conferences (WCNC'99 and WCNC'00), the 1999 IEEE International Workshop on Intelligent Signal Processing and Communication Systems (ISPACS'99), the EuroComm 2000 Conference, and the 2000 Spring IEEE Vehicular Technology Conference (VTC'00 Spring). He also serves on the Organizing Committees of the 2000 IEEE International Symposium on Circuits & Systems (ISCAS'00) and the Symposium 2000 on Adaptive Signal Processing, Communications and Control (AS-SPCC).

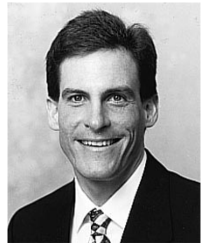

Michael D. Zoltowski (S'79–M'86–SM'95–F'99) was born in Philadelphia, PA, on August 12, 1960. He received the B.S. and M.S. degree in electrical engineering (with highest honors) from Drexel University, Philadelphia, in 1983 and the Ph.D. degree in systems engineering from the University of Pennsylvania, Philadelphia, in 1986.

From 1982 to 1986, he was an Office of Naval Research Graduate Fellow. In the fall of 1986, he joined the faculty of Purdue University, West Lafayette, IN, where he currently holds the position of Professor of Electrical and Computer Engineering. During 1987, he held a position of Summer Faculty Research Fellow at the Naval Ocean Systems Center, San Diego, CA. He is a contributing author to *Adaptive Radar Detection and Estimation* (New York: Wiley, 1991), *Advances in Spectrum Analysis and Array Processing, Vol. III* (Englewood Cliffs, NJ: Prentice-Hall, 1994), and *CRC Handbook on Digital Signal Processing* (Boca Raton, FL: CRC Press, 1996). His present research interests include space–time adaptive processing coding for all areas of mobile and wireless communications, GPS, and radar.

Dr. Zoltowski is currently a Member-at-Large of the Board of Governors and Secretary of the IEEE Signal Processing Society, for which he has been a member of the Technical Committee for the Statistical Signal and Array Processing Area and is currently a member of both the Technical Committee for Communications and the Technical Committee on DSP Education. He has served as an Associate Editor for both the IEEE TRANSACTIONS ON SIGNAL PROCESSING and the IEEE COMMUNICATIONS LETTERS.